Chapter 7
Engine Limit Management with Linear Regulators

Abstract This chapter describes the min–max logic arrangement used in standard engine control systems to maintain critical variables within the permissible bounds. A thorough analysis of this arrangement is conducted using the concept of positive invariance. The shortcomings of the min–max approach are made evident in simulations. A brief description of an acceleration-limiting approach is also included.

The control techniques presented so far do not address the need to maintain critical engine variables within permissible limits. As described in Sect. 1.3, engine outputs such as stall margins and turbine temperatures must be kept between safe limits at all times. The values chosen for safety limits depend on particular engine characteristics, and typically reflect a tradeoff between high engine performance and engine durability and operational safety. Indeed, large shaft accelerations are desirable for improved maneuverability, since they produce fast thrust responses to pilot commands. Large accelerations lead to transient reductions in stall margin, however, increasing the danger of compressor surge. Large accelerations also correlate with large turbine temperature transients. Since blade wear rate increases with temperature, transient peak temperature suppression should be included as an objective when designing fan speed controllers.

Constraints can be placed on system inputs and outputs. Temperatures, stall margins, and pressure ratios are examples of output variables that may be subject to constraints as part of a particular design process. Fuel flow rates and VSV and VBV openings are inputs whose ranges are constrained. Input constraints can arise from the same considerations as output constraints, that is, to address engine durability or safety, or from the presence of physical limits in actuator systems. An example of a safety-related input constraint is a minimum fuel flow rate requirement, imposed to maintain the combustion chamber away from lean blowout conditions. An example of a physical actuator constraint is given by the fact that a valve may not be more than 100% open or less than fully closed. When such *actuator saturation* effects are ignored during controller design, the implemented closed-loop controller may oscillate or even become unstable. Designs which do not explicitly address

saturation must be validated via simulation studies to evaluate the possibility and effects of saturation modes during real-time operation.

In this chapter, a widely used control architecture intended to achieve limit protection is examined. The *min–max* approach, presented in Sect. 7.1, is used in many GTE control systems. CMAPSS-1 and CMAPSS-40k are distributed with min–max limit management implementations, representative of the actual control systems used in commercial engines such as General Electric's GE90 and Pratt and Whitney's PW2000.

The concept of set invariance is introduced in Sect. 7.2. This concept is instrumental to the analysis of constrained control systems in general. Some basic invariant set constructions are presented to illustrate the application of the theory to GTE control. In Sect. 7.3, min–max architecture based on state feedback controllers is analyzed for its invariance properties. Detailed examples using the CMAPSS-1 model are given throughout the chapter.

7.1   The Min–Max Limit Management Logic

The *min–max* selector arrangement is representative of actual aircraft engine control systems. Similar arrangements have also been used in industrial processes where a number of system outputs must be kept between prescribed limits as a main output is controlled between setpoints. *The premise is that a single control input is available for the tasks of controlling the main output and maintaining a set of outputs between desired limits*. Figure 7.1 shows the min–max arrangement with
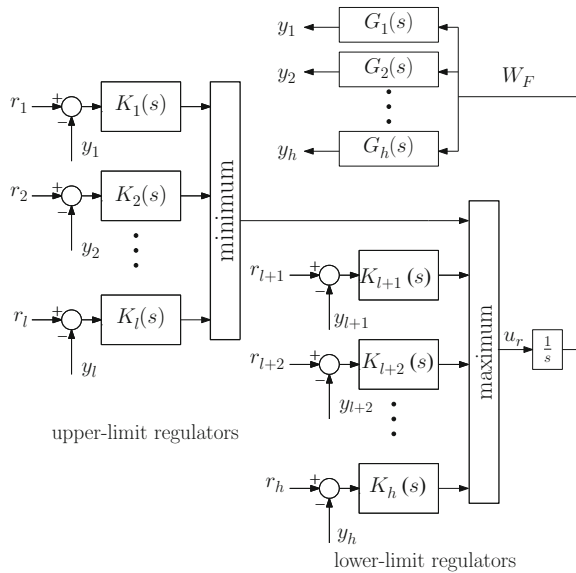

Fig. 7.1 Min–max limit management logic with linear compensators and integral control

linear compensators. A version of the min–max arrangement with state feedback controllers is used for analysis in Sect. 7.3, and a version replacing the linear compensators with sliding mode controllers is presented in Chap. 8.

As shown in Fig. 7.1, the technique uses input integration. The fuel flow control input W_F is applied to the engine, resulting in a set of h outputs characterized by their linearized transfer functions from W_F. Outputs are divided into two groups: a set of *upper-limited outputs*, numbered as y_i, for $i = 1, 2...l$ and a set of *lower-limited outputs*, numbered with $i = l + 1, l + 2, ...h$. The reader should note that transfer functions $G_i(s)$ for $i = 1, 2...h$ share the same poles, since they arise from the same linearized state-space matrix A. The static gains $G_i(0)$ and zero locations will differ, due to differences in matrices C and D defining the outputs. It is also useful to remember that GTE dynamics are such that neither the transfer functions $G_i(s)$ nor A have poles at the origin.

The min–max system is conceived to prevent selected variables from crossing their limits, by activating their regulators as needed. If a variable approaches its limit, its regulator should take over and attempt to drive the output to the prescribed limit without overshooting it. The diagram of Fig. 7.1 shows that upper-limited variables $y_i(s)$ each have a controller $K_i(s)$ with a classical error feedback structure. The setpoint corresponds to the desired output limit, r_i. Each upper-limited controller produces a "candidate" control rate u_{ri}. The minimum rate among upper-limit regulator outputs is preliminarily chosen. A separate set of lower-limit controllers produce their own candidate control rates. The maximum control rate among lower-limit regulator rates and the "winner" from the min stage is selected as the rate to be integrated, producing the fuel flow input command applied to the plant.

The above description cannot be expected to satisfy the average controls engineer. Unfortunately, few works can be found in the open literature that conduct a detailed analysis of this system. Is the system always stable? Could it produce endless switching among regulators? Why are upper-limited variables associated with the min selector and lower-limited variables to the max selector? Under which conditions is limit preservation guaranteed? It turns out that some of these questions have simple and thorough answers, while others are either unresolved or require analysis beyond the scope of this book.

The question of stability of min–max implementations using linear regulators, for instance, has been treated with nonlinear techniques applicable to sector-bounded nonlinearities, such as Popov's criterion and the famous Small Gain Theorem (see Glattfelder and Schaufelberger [58], for instance). These tools provide only sufficient conditions, resulting in very conservative stability assessments. Johansson [33] has analyzed a conceptually similar system using the tools of piecewise-linear systems and multiple Lyapunov functions.

The author of this book proposed that the linear regulators be replaced by sliding mode controllers. Although analysis becomes more complex due to the nonlinearity inherent to sliding mode control, a full global asymptotic stability proof was achieved and simple design guidelines generated, see Richter [59]. This is presented in Chap. 8.

The question of limit protection effectiveness is difficult to establish for the transient regime when dynamic compensators (control transfer functions) are used. When static feedback laws of the form $u = -Kx + Pr$ are used instead, some simplifications occur, facilitating analysis. In the following sections, the dynamic compensation case is studied for its limit protection properties at steady-state only, while the static feedback case is analyzed for both transient and steady-state limit preservation properties.

7.1.1 Default Index Assumptions: Min and Max Operators

Although the generic mathematical operations of taking the minimum or maximum require no explanations, assumptions must be made regarding their behavior in the event of non-unique minimum or maximum values among operands. For the remainder of the book, we adopt the assignment rules made by the min and max operations implemented in many computer languages. Let $\{N(i)\}$ represent an indexed collection of real numbers, for $i = 1, 2, \ldots n$ and let $\bar{N}$ and $\underline{N}$ denote, respectively, the maximum and minimum values found in the collection. If there exists a single index $\bar{i}$ such that $N(\bar{i}) = \bar{N}$, $\bar{i}$ is chosen as the outcome of the max selection process. In general, if a set of maximizing indices exists, that is set $\{I(j)\}$ is such that $N(I(j)) = \bar{N}$, then the lowest of such indices is chosen: $\bar{i} = \min(I(j))$. For example, take the set $N = \{3, 5, -2, 5, 5, -2\}$. Here, $\bar{N} = 5$ and $I = \{2, 4, 5\}$, thus $\bar{i} = 2$. A similar convention is adopted for the min selector. In the same example, $\underline{i} = 3$. This convention will be referred to as *default index assumption* in what follows.

7.1.2 Static Properties of the Min–Max Arrangement with Dynamic Compensators

Three fundamental questions pertaining to the operation of the min–max arrangement are decided next: determining the regulator that becomes active at the initial time ($t = 0$), determining the regulator that remains active during a steady-state regime ($t \to \infty$), and establishing conditions for limits to be preserved at steady-state. As shown later in the chapter, a min-only or a max-only arrangement is sufficient in some cases. Because of this and to facilitate understanding, analysis is separated into min-only, max-only, and min–max cases.

7.1.2.1 Initial Regulator: Min-Only Case

Suppose only the min selector is used to select a control rate u_r among candidate rates $u_{ri}, i \in L$. The min selection law is expressed as

$$u_r = \min_{i \in L} \{u_{ri}\}. \tag{7.1}$$

Suppose $i = i_0$ is the regulator at the initial time. Then the following inequality must hold for all j:

$$u_{ri_0}(0) \leq u_{rj}(0).$$

If there exists $j \neq i_0$ such that $u_{rj} = u_{ri_0}$, then it is necessary that $i_0 < j$ due to the default index assumptions. The control rates are expressed in terms of transfer functions as

$$U_{ri_0}(s) = \frac{K_{i_0}(s)}{1 + G'_{i_0}(s)K_{i_0}(s)} R_{i_0}(s), \tag{7.2}$$

$$U_{rj}(s) = K_j(s)(R_j(s) - G_j(s)U_{ri}(s)), \tag{7.3}$$

where $G'_{i_0}(s) = G_{i_0}(s)/s$. Recalling the *initial value theorem* [26] and noting that $R_{i_0}(s) = r_{i_0}/s$ and $R_j(s) = r_j/s$, we have

$$u_{ri_0}(0) = \lim_{s \to \infty} sU_{ri_0}(s) = \lim_{s \to \infty} \frac{r_i K_{i_0}(s)}{1 + G'_{i_0}(s)K_{i_0}(s)}. \tag{7.4}$$

Note that G'_{i_0} has a pole at $s = 0$ and that it is strictly proper, since G_{i_0} is proper and does not have zeroes at $s = 0$. Therefore, if $K_{i_0}(s)$ is proper, we have $u_{ri_0}(0) = K_{i_0}(\infty)r_{i_0}$. When $K_{i_0}(s)$ is an improper PD transfer function, the derivative term is impulsive when r_{i_0} is constant. The initial regulator observed in simulations or real-time deployments will depend on the approximation involved in the implementation of the derivative term. Therefore, we restrict our formulas for the initial regulator to the case when all controllers are proper.

Now, using the initial value theorem on u_{rj}, we have

$$u_{rj}(0) = \lim_{s \to \infty} sU_{rj}(s) = \lim_{s \to \infty} \left\{ r_j K_j(s) - sG_j(s)U_{ri_0}(s) \right\}. \tag{7.5}$$

The reader can verify that if $K_j(s)$ is proper $u_{rj}(0)$ has a well-defined constant value:

$$u_{rj}(0) = K_j(\infty)r_j.$$

Therefore, the initial regulator is calculated as the smallest index i_0 satisfying

$$K_{i_0}(\infty)r_{i_0} \leq K_j(\infty)r_j \tag{7.6}$$

for all $j \in L$.

7.1.2.2   Initial Regulator: Max-Only Case

Now consider that only the max selector is used to select a control rate u_r among candidate rates u_{ri}, $i \in H$. The max selection law is expressed as

$$u_r = \max_{i \in H} \{u_{ri}\}. \tag{7.7}$$

Suppose $i = i_0$ is the regulator at the initial time. The initial values of the rates u_{ri} are the same regardless of the type of selector, max or min. The initial selection is therefore given by the smallest index i_0 satisfying

$$K_{i_0}(\infty)r_{i_0} \geq K_j(\infty)r_j \tag{7.8}$$

for all $j \in H$.

7.1.2.3   Initial Regulator: Min–Max Case

The min–max case has a subtlety that requires careful attention. Referring back to Fig. 7.1, the min–max selection law is given by

$$u_r = \max_{k \in H} \left\{ \min_{j \in L} \{u_{rj}\}, \ u_{rk} \right\}, \tag{7.9}$$

where u_{rj} are the min-selected regulator outputs and u_{rk} are the max-selected regulator outputs. Again, the values of the initial rates are the same regardless of the selection mechanism. Suppose i_0 is the index of the regulator selected at $t = 0$. If $i_0 \in L$, the following inequalities must be true:

$$u_{ri_0} \leq u_{rj} \text{ for all } j \in L, \tag{7.10}$$

$$u_{ri_0} \geq u_{rk} \text{ for all } k \in H. \tag{7.11}$$

If $i_0 \in H$, however, the following inequalities apply:

$$u_{ri_0} > u_{rk} \text{ for all } k \in L, \tag{7.12}$$

$$u_{ri_0} > \min_{j \in L} \{u_{rj}\}. \tag{7.13}$$

Note that strict inequality must be used, since the winner of the min stage is applied to the first port of the max selector. Thus, equality between the winner of the max stage and the winner of the min stage would result in $i_0 \in L$ due to the default index assumptions. Also note that u_{ri_0} is required to be greater than the *minimum* of the rates produced by regulators in L, but not necessarily greater than each. This implies that a two-step iterative process must be followed to determine i_0. Assume first that

$i_0 \in L$ and find the smallest index satisfying inequalities (7.10) and (7.11). If no such index can be found, it must be that $i_0 \in H$. Inequalities (7.12) and (7.13) are then tested using the known value of the winner of the min stage.

The reader should observe that the calculations for the initial regulator in the min, max and min–max cases are not influenced by whether a variable is upper- or lower-limited. Only the type of selector must be taken into account.

7.1.2.4 Steady Regulator: Min-Only Case

Here, we assume that the closed-loop system is asymptotically stable, with a fixed steady-state regulator selection denoted as i^*. Applying the *final value theorem* [26] to the Laplace expression for the control rate of (7.2), we obtain

$$u_{ri^*}(\infty) = \lim_{s\to 0} sU_{ri^*}(s) = \lim_{s\to 0} \frac{r_{i^*}K_{i^*}(s)}{1 + G'_{i^*}(s)K_{i^*}(s)}. \qquad (7.14)$$

The reader can verify that $u_{ri^*} = 0$ whenever K_{i^*} and G_{i^*} are proper and do not have zeroes at the origin. Furthermore, the same is true if K_{i^*} is a PD transfer function and G_{i^*} is proper with no zeroes at the origin. This is expected, since the active loop is of type I, and the steady-state error to constant inputs is zero. Since K_{i^*} is driven by the error, its output will be zero at steady-state.

Applying the final value theorem to $U_{rj}(s)$ from (7.3), we obtain

$$u_{rj}(\infty) = \lim_{s\to 0} sK_j(s)\left[\frac{r_j}{s} - G_j(s)U_{ri^*}(s)\right].$$

If $G_j(s)$ and $K_j(s)$ are proper with no poles at the origin, this reduces to

$$u_{rj}(\infty) = K_j(0)\left[r_j - r_i\frac{G_j(0)}{G_{i^*}(0)}\right]. \qquad (7.15)$$

Therefore, i^* is the smallest index satisfying

$$K_j(0)\frac{r_{i^*}G_j(0)}{G_{i^*}(0)} \leq K_j(0)r_j, \qquad (7.16)$$

for all $j \in L$. Note that

$$\frac{r_{i^*}G_j(0)}{G_{i^*}(0)} = \bar{y}_{j/i^*},$$

where $\bar{y}_{j/i^*}$ is the steady value attained by y_j when i^* is the steady regulator. If $K_j(0) > 0$, inequality (7.17) reduces to $\bar{y}_{j/i^*} \leq r_j$. This is interpreted verbally as follows: "i^* is the regulator for which outputs do not exceed their setpoints at steady-state". If $K_j(0) < 0$, the inequality becomes $\bar{y}_{j/i^*} \geq r_j$. This corresponds to: "i^* is the regulator for which outputs do not become smaller than their setpoints at steady-state".

7.1.2.5 Steady Regulator: Max-Only Case

The final regulator index for this case is the smallest index i^* satisfying

$$K_j(0)\frac{r_{i^*}G_j(0)}{G_{i^*}(0)} \geq K_j(0)r_j \qquad (7.17)$$

for all $j \in H$. If $K_j(0) > 0$, inequality (7.17) reduces to $\bar{y}_{j/i^*} \geq r_j$. This is interpreted verbally as follows: "i^* is the regulator for which outputs do not become smaller than their setpoints at steady-state". If $K_j(0) < 0$, the inequality becomes $\bar{y}_{j/i^*} \leq r_j$. This corresponds to: "i^* is the regulator for which outputs do not exceed their setpoints at steady-state".

The steady properties of the isolated min and max selectors provide a basic guideline for design. If all outputs are upper-limited and $K_j(0) > 0$ for all j, a max regulator provides steady-state limit protection. If all outputs are lower-limited and $K_j(0) > 0$ for all j, a max selector provides steady-state limit protection. This seems to be the assumption justifying the assignments found in the standard min–max arrangements used in the aerospace industry.

As the reader may appreciate, the more general case where outputs have different signs of $K_j(0)$, some being lower-limited and some being upper-limited are not covered by the min-only or max-only arrangements. The min–max arrangement was introduced as an attempt to cover these cases.

7.1.2.6 Steady Regulator: Min–Max Case

The same logic used for determining the initial regulator is followed, using the appropriate formulas for the steady rates. If $i^* \in L$, the following inequalities hold:

$$0 \leq u_{rj} \text{ for all } j \in L, \qquad (7.18)$$

$$0 \geq u_{rk} \text{ for all } k \in H. \qquad (7.19)$$

If $i^* \in H$, however, the following inequalities apply:

$$0 > u_{rk} \text{ for all } k \in L, \qquad (7.20)$$

$$0 > \min_{j \in L}\{u_{rj}\}. \qquad (7.21)$$

7.1.3 Example: CMAPSS-1

Consider the transfer functions from incremental fuel flow to incremental fan speed (rpm), incremental HPT temperature (°R) and HPC stall margin (%) near FC01:

$$G_1(s) = \frac{\Delta N_f(s)}{\Delta W_F(s)} = \frac{230.9s + 2000}{s^2 + 8.504s + 17.16},$$

$$G_2(s) = \frac{\Delta T_{48}(s)}{\Delta W_F(s)} = \frac{146.2s^2 + 1027s + 1528}{s^2 + 8.504s + 17.16},$$

$$G_3(s) = \frac{\Delta SmHPC(s)}{\Delta W_F(s)} = \frac{-4.405s^2 - 28.81s - 20.49}{s^2 + 8.504s + 17.16}.$$

Suppose that a set of controllers is selected that independently stabilize the above transfer functions under an integral control loop (disregarding transient response qualities), as follows:

$$K_1(s) = 0.21\frac{s + 3.715}{s + 20},$$

$$K_2(s) = 0.1,$$

$$K_3(s) = \frac{-s - 1}{s + 2}.$$

Suppose $r_1 = 10$, $r_2 = 20$, and $r_3 = -10$. In this example, $G_1(\infty) = 0$, $G_2(\infty) = 146.2$ and $G_3(\infty) = -4.405$. Also, $K_1(\infty) = 0.21$, $K_2(\infty) = 0.1$, and $K_3(\infty) = -1$. Similarly, $G_1(0) = 116.55$, $G_2(0) = 89.044$, $G_3(0) = -1.194$ and $K_1(0) = 0.039$, $K_2(0) = 0.1$ and $K_3(0) = -0.5$.

If only a min selector is used, (7.6) can be used to determine that the initial regulator is $i_0 = 2$ and the final regulator is $i^* = 1$. If only a max selector is used, $i_0 = i^* = 3$. Suppose now that u_{r1} and u_{r2} are associated with a min selector, while the min-preselection and u_{r3} are associated with a max selector. It can be readily verified that $i_0 = i^* = 3$ as well.

The concept of *positive invariance* is introduced next as an essential tool to study limit regulator behavior.

7.2 Basic Set Invariance Concepts

Set invariance theory is a unifying umbrella under which many techniques for constraint handling have been developed. Although a detailed account of set invariance and derived techniques is out of the scope of this book, some definitions and results will be included. For an excellent introduction to the topic, readers are referred to the survey by Blanchini [60].

Given a dynamical system with state vector x, a *positively invariant* set is a subset S_o of the state-space formed by all initial conditions resulting in trajectories, which remain in S for all subsequent times. That is, S_o is positively invariant if $x(0) \in S_o$ implies $x(t) \in S_o$ for all $t > 0$, justifying the *positive* invariance qualification.

A result by Nagumo [61] establishes a necessary and sufficient condition for a set to be positively invariant with respect to a given dynamical system. For the purposes

Fig. 7.2 Illustration
of Nagumo's invariance
condition. $\mathcal{S}_o$ is the invariant
set and $\partial \mathcal{S}_o$ its boundary
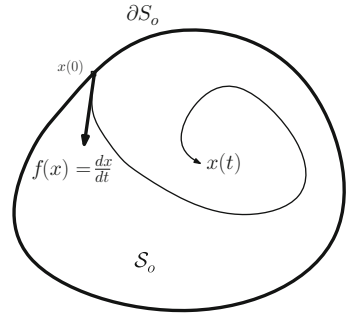
of this book, invariant sets of simple descriptions are considered, such as ellipsoids,
half-spaces, and real intervals. Roughly, Nagumo's condition is equivalent to the
requirement that the vector $\dot{x}$ evaluated along the boundary of $\mathcal{S}_o$ be directed toward
its interior, as illustrated in Fig. 7.2. Nagumo's condition is rather intuitive, and
becomes more so when x is a scalar, so that the invariant set is an interval, as shown
next.

7.2.1 Positive Invariance of an Interval

An interval $(-\infty, b]$ is invariant for a generic real variable $z(t)$ if $\dot{z}(t) \leq 0$ at $z = b$.
Similarly, an interval $[a, \infty)$ is invariant if $\dot{z}(t) \geq 0$ at $z = a$. When an interval is
invariant and $z(t_1)$ belongs to the interval for some $t_1 > 0$, then $z(t)$ will remain in
the interval for $t \geq t_1$. The concept is readily applied to limit protection: the interval
$(-\infty, 0]$ must be invariant for the error $e = r - y$ when y is a lower-limited output.
Conversely, $[0, \infty)$ must be invariant for the error of upper-limited variables.

7.2.2 Ellipsoidal Invariant Sets for Linear Systems

An n-dimensional ellipsoid is described by the inequality

$$x^\mathrm{T} P x \leq 1,$$

where P is a symmetric, positive-definite matrix. Consider first an autonomous
linear state-space system described $\dot{x} = Ax$ and an ellipsoidal set $\mathcal{S}_o$ described as

$$\mathcal{S}_o = \mathcal{E} = \{x \; : \; x^\mathrm{T} P x \leq 1\}.$$

For $\mathcal{E}$ to be PI, Nagumo's theorem requires that $\dot{x} = f(x) = Ax$ be directed toward
the interior of $\mathcal{E}$, when x is taken at its boundary, defined by $h(x) = x^\mathrm{T} P x = 1$.

Fig. 7.3 Invariance enforcement by negative gradient projection
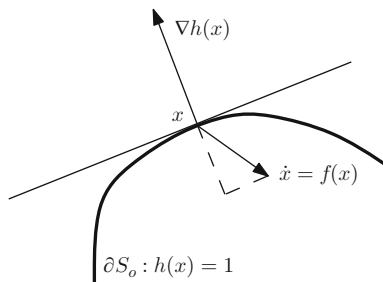
This can be ensured by the condition that the projection of $f(x)$ onto a vector normal to the boundary be negative, as shown in Fig. 7.3. The invariance condition is expressed as

$$\nabla h(x).f(x) < 0.$$

For an ellipsoidal boundary we have $\nabla h(x) = 2x^{\mathrm{T}}P$, thus the condition becomes $2x^{\mathrm{T}}PAx < 0$. The reader may recall that any square matrix can be decomposed into a symmetric component and an antisymmetric component. Decompose PA as follows:

$$PA = \frac{1}{2}(PA + A^{\mathrm{T}}P) + \frac{1}{2}(PA - A^{\mathrm{T}}P).$$

The first term is symmetric, while the second is antisymmetric. Thus,

$$2x^{\mathrm{T}}PAx = x^{\mathrm{T}}(PA + A^{\mathrm{T}}P)x + x^{\mathrm{T}}(PA - A^{\mathrm{T}}P)x.$$

Recalling that the cross-terms of a quadratic form $xY^{\mathrm{T}}x$ cancel out when Y is antisymmetric, the invariance condition reduces to the following *Lyapunov inequality*

$$PA + A^{\mathrm{T}}P < 0. \tag{7.22}$$

The above condition can be applied to evaluate the invariance of an ellipsoid relative to the closed loop system $\dot{x} = (A - BK)x$ resulting from using the state feedback control law $u = -Kx$:

$$P(A - BK) + (A - BK)^{\mathrm{T}}P < 0. \tag{7.23}$$

Note that inequality (7.23) is satisfied *for some* P when K stabilizes $A - BK$, but that a predetermined P need not satisfy the inequality for all stabilizing K. A family of invariant ellipsoids associated with a given stabilizing K can be found by turning inequality (7.23) into equality, using an arbitrary positive-definite, symmetric matrix Q:

$$P(A - BK) + (A - BK)^{\mathrm{T}}P = -Q. \tag{7.24}$$

All ellipsoids of the form $x^{\mathrm{T}}Px = a$, with $a \geq 0$ are then PI relative to the closed-loop dynamics.

7.2.3 Invariance of a Half-Space

State and output constraints can be formulated as a set of linear inequalities in the state variables: $\mathcal{G} = \cap \mathcal{G}_i$ for $i = 1, 2..m$, where $\mathcal{G}_i = \{x : G_i x \leq 1\}$. Application of Nagumo's result to a system $\dot{x} = f(x)$ and an individual linear constraint $G_i x \leq 1$ results in the following condition for invariance:

$$G_i f(x) \leq 0 \text{ along } G_i x = 1. \tag{7.25}$$

In the case of a linear state-space system (A, B) under state feedback $u = -Kx$, this reduces to

$$G_i (A - BK)x \leq 0 \text{ along } G_i x = 1. \tag{7.26}$$

In general, condition (7.26) cannot be satisfied for all points belonging to the boundary defined by $G_i x = 1$. Geometrically, if G_i is not parallel to $G_i (A - BK)$, the boundary will be divided into three subsets: a subset where $G_i (A - BK)x = 0$, a subset where $G_i (A - BK) > 0$ and a subset where the condition is satisfied. When several constraints exist, methodologies have been developed to ensure that points belonging to the set, where $G_i (A - BK)x > 0$ do not satisfy the other constraints. *Polyhedral invariant set theory* provides means to construct invariant sets using linear segments. Given a constraint set defined by design requirements, polyhedral invariant sets can be constructed with little conservativeness. An invariant set construction is conservative if it excludes points of the constraint set which actually lead to permissible trajectories. Polyhedral sets require a large number of vertices to achieve low conservativeness. The interested reader is referred to Blanchini's survey for an introduction [60].

7.2.4 Ellipsoidal Operating Sets

Invariant sets are used to determine the range of allowable initial conditions so that the ensuing trajectories do not violate the constraints. When error dynamics are used as a basis, an invariant set description can be used to determine the allowable range of the setpoints so that no limit violations will occur in the transient or steady regimes. Such *operating sets* are thus invariant subsets of the constraint set. A simple approach to finding an operating set is to find the largest invariant ellipsoid contained in the constraint set. For this, ellipsoids which are tangent to individual constraints are found. The smallest of such ellipsoids will be tangent to one of the constraints and tangent or interior to the remaining ones, in addition to being invariant.

Given a linear constraint $G_i x \leq 1$, and an invariant ellipsoid family defined by matrix P, the ellipsoid which is tangent to the boundary $G_i x = 1$ can be found by solving the following constrained optimization problem:

$$\max V = x^T P x \text{ subject to}$$

$$G_i x = 1.$$

This is readily solved using Lagrange multipliers, yielding the following formula for the maximum value of $x^{\mathrm{T}} P x$:

$$V_i = \frac{1}{G_i P^{-1} G_i^{\mathrm{T}}}.$$

Thus, the largest invariant ellipsoid tangent to the i-th constraint is given by

$$\mathcal{E}_i = \{x \ : \ x^{\mathrm{T}} P x \le V_i\},$$

where P satisfies inequality (7.24). The overall invariant ellipsoid can be found by taking the smallest V_i and matrix P. As an introductory example, consider the double-integrator plant $G(s) = 1/s^2$ with state-space matrices A and B as follows:

$$A = \begin{bmatrix} 0 & 1 \\ 0 & 0 \end{bmatrix}, \quad B = \begin{bmatrix} 0 \\ 1 \end{bmatrix}.$$

Suppose the constraints are given by $|x_1| \le 1$ and $|x_2| \le 1.5$. The plant is stabilized with a state-feedback law of the form $u = -Kx$, where K is chosen so that $A_{\mathrm{c}} = A - BK$ has eigenvalues with negative real parts. Suppose a K is designed using an LQR approach, with $Q = I$ and $R = 1$. This yields $K = [1 \ \sqrt{3}]$, which places the poles of A_{c} at $-\sqrt{3}/2 \pm i/2$. The following P satisfies Lyapunov inequality (7.23):

$$P = \begin{bmatrix} 1.5847 & 0.5489 \\ 0.5489 & 0.6339 \end{bmatrix}.$$

The constraints are expressed as $G_1 x = [1 \ 0]x \le 1$, $G_2 x = [-1 \ 0]x \le 1$, $G_3 x = [0 \ 1/1.5]x \le 1$ and $G_4 = [0 \ -1/1.5]x \le 1$. The values of V_i are calculated as $V_1 = V_2 = 1.109$ and $V_3 = V_4 = 1$. Thus, the ellipsoid described by $x^{\mathrm{T}} P x \le 1$ is tangent the third and fourth constraints and interior to the first and second constraints, in addition to being positively invariant. Figure 7.4 shows the ellipsoidal boundary in relation to the constraints. A few trajectories have also been plotted.

The dotted line represents a trajectory which satisfies the constraints but whose initial condition is not captured by the ellipsoid. In contrast, the dashed line is a trajectory whose initial point belongs to the constraint set but which produces constraint violation, and is correctly excluded by the ellipsoidal set. An example of the ellipsoidal construction as applied to the GTE problem is given in Sect. 7.5.2.

A less conservative invariant set construction which retains the simplicity of ellipsoids is given by the semiellipsoidal approach of O'Dell [62]. In this approach, an invariant ellipsoid which may exceed the constraints is sought under the condition that its intersection with the constraints retains the positive invariance property. The methodology regards K and P as free parameters, optimized to yield an ellipsoid of maximum volume. The resulting semiellipsoidal set is an approximation to the maximal recoverable set under state feedback, i.e., the largest set of initial conditions yielding trajectories which proceed to the origin without constraint violation. The maximizing argument K does not offer any performance guarantees, however.
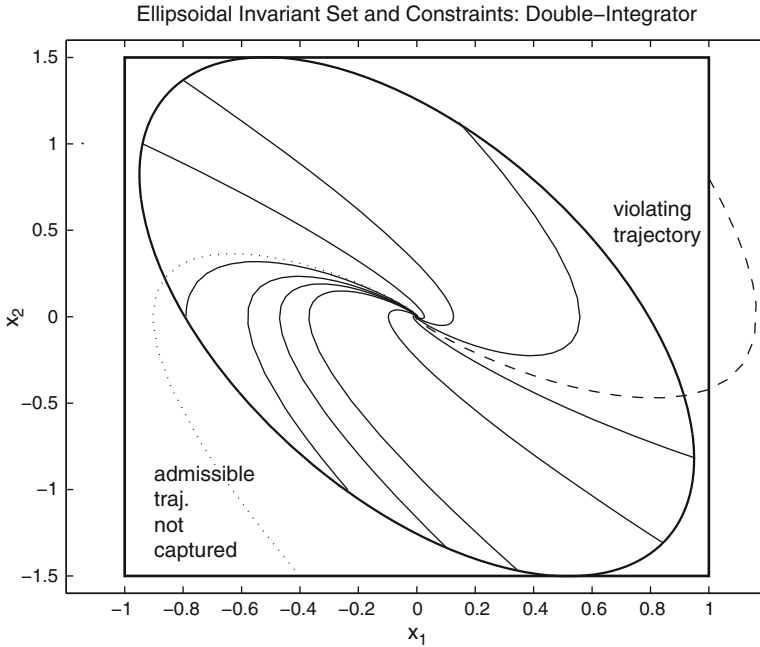
Ellipsoidal Invariant Set and Constraints: Double–Integrator

Fig. 7.4 Ellipsoidal invariant set and constraints: double-integrator system

The operating set approach amounts only to "passive" constraint validation. If invariance cannot be established without unreasonable conservativeness, a different control law must be found or the constraints relaxed. In contrast, approaches such as the min–max arrangement constitute *active* means to enforce the constraints as the system operates. The use of a *reference governor* allows to exploit set invariance properties in an active way. The key idea is to filter reference inputs to force the state to remain in an invariant set, see, for instance, Bemporad [63].

7.3 Min–Max Limit Management with Integral State Feedback Controllers

Analysis of the min–max arrangement is somewhat simplified when state feedback controllers are used instead of dynamic compensators. Consider a linear plant with input integration, described by the following augmented state-space model:

$$\dot{x}_a = A_a x_a + B_a u_r, \tag{7.27}$$

$$y_i = C_{ai} x_a, \tag{7.28}$$

where $x_a^T = [x^T \ u]$ is the augmented state vector and A_a and B_a are defined as in (4.31). Outputs $y_i = C_i x + Du$ are defined by their augmented matrices $C_{ai} = [C_i \ D_i]$. Consider the static state feedback law

$$u_{ri} = -K_i x_a + P_i r_i, \tag{7.29}$$

where K_i is such that $A_a - B_a K_i$ is stable. Although K_i could be chosen to be constant across regulators to guarantee stability and achieve desirable transient properties for the main controlled output, the min–max arrangement would become useless. To see this, note that $u_{ri} - u_{rj}$ is constant for a given pair i, j when a constant K is used. Thus, the regulator selected by min and max at $t = 0$ becomes permanent and no switching occurs. Assume, then, that the min, max, and min–max arrangements involve distinct feedback gains.

The value of the *prefilter gain* P_i is chosen to ensure that $y_i = r_i$ in the steady-state, and must therefore vary with i (see (7.35)).

7.3.1   Closed-Loop Behavior Under a Fixed Regulator

Suppose the i-th regulator is active at all times. The closed-loop system becomes

$$\dot{x}_a = A_{ci} x_a + B_a P_i r_i, \tag{7.30}$$

where $A_{ci} = A_a - B_a K_i$. Since K_i is designed so that A_{ci} has eigenvalues with negative real parts, the augmented state reaches a steady-state value of $\bar{x}_{ai}$ satisfying

$$0 = A_a \bar{x}_{ai} + B_a \bar{u}_{ri}, \tag{7.31}$$

$$0 = \bar{u}_{ri} = -K_i \bar{x}_{ai} + P_i r_i, \tag{7.32}$$

where (7.32) is obtained from the requirement that the last component of the augmented state derivative be zero at steady-state, that is, $\dot{u} = \bar{u}_{ri} = 0$. Equations (7.31) and (7.32) imply that $A_a \bar{x}_{ai} = 0$ and that P_i must be related to $\bar{x}_{ai}$ as follows:

$$P_i = K_i \frac{\bar{x}_{ai}}{r_i}. \tag{7.33}$$

The value of $\bar{x}_{ai}$ is determined by the requirement that $y_i = r_i$ at steady-state. Separating the first n components of (7.31), we have:

$$0 = A\bar{x} + B\bar{u},$$

where $\bar{x}_{ai}^T = [\bar{x}^T \ \bar{u}]$. Since A has no poles at the origin, $\bar{x} = -A^{-1}B\bar{u}$. The steady output is then

$$\bar{y}_i = C_i \bar{x} + D_i \bar{u} = (-C_i A^{-1} B + D_i)\bar{u} = G_i(0) r_i.$$

For $\bar{y}_i = r_i$, we must have $\bar{u} = r_i/G_i(0)$ and $\bar{x} = -A^{-1}Br_i/G_i(0)$, thus

$$\bar{x}_{ai} = \frac{r_i}{G_i(0)}\begin{bmatrix} -A^{-1} & B \\ & 1 \end{bmatrix}, \tag{7.34}$$

$$P_i = \frac{K_i}{G_i(0)}\begin{bmatrix} -A^{-1} & B \\ & 1 \end{bmatrix}. \tag{7.35}$$

7.3.2 Closed-Loop Behavior Relative to a Fixed Index

It is convenient to shift the augmented state variable by the steady-state value corresponding to an arbitrary index i. That is, define

$$\tilde{x}_{ai} = x_{ai} - \bar{x}_{ai}. \tag{7.36}$$

Relevant quantities are now expressed in terms of $\tilde{x}_{ai}$. The i-th and j-th outputs become

$$y_i = C_{ai}x_a = C_{ai}(\tilde{x}_{ai} + \bar{x}_{ai}) = r_i + C_{ai}\tilde{x}_{ai}, \tag{7.37}$$

$$y_j = C_{aj}x_a = C_{aj}(\tilde{x}_{ai} + \bar{x}_{ai}) = \bar{y}_{j/i} + C_{aj}\tilde{x}_{ai}, \tag{7.38}$$

where $\bar{y}_{j/i}$ is the steady value of y_j when i is active at steady-state. The tracking errors are expressed in terms of the new state variable as

$$e_i = r_i - y_i = -C_{ai}\tilde{x}_{ai}, \tag{7.39}$$

$$e_j = r_j - y_j = \bar{e}_{j/i} - C_{aj}\tilde{x}_{ai}, \tag{7.40}$$

where $\bar{e}_{j/i}$ denotes the steady-state error in y_j when i is active. The control rates are expressed as

$$u_{ri} = -K_i(\tilde{x}_{ai} + \bar{x}_{ai}) + P_i r_i = -K_i\tilde{x}_{ai}, \tag{7.41}$$

$$u_{rj} = -K_j(\tilde{x}_{ai} + \bar{x}_{ai}) + P_j r_j, \tag{7.42}$$

where (7.32) has been used.

The reader should observe that (7.37)–(7.42) use an arbitrary index i as a reference, but are valid regardless of the active regulator. The next two expressions for the derivatives of tracking errors e_i and e_j, however, assume that i is the active regulator, and this is reflected in the notations $\dot{e}_{i/i}$ and $\dot{e}_{j/i}$.

$$\dot{e}_{i/i} = -C_{ai}A_{ci}\tilde{x}_{ai}, \tag{7.43}$$

$$\dot{e}_{j/i} = -C_{aj}A_{ci}\tilde{x}_{ai}. \tag{7.44}$$

Equations (7.30) and (7.31), and the definition of $\tilde{x}_{ai}$ from (7.36) have been used in the derivation of (7.43) and (7.44). Finally, the following expression for the difference between control rates will be useful in subsequent developments:

$$u_{ri} - u_{rj} = (K_j - K_i)\tilde{x}_{ai} + K_j\bar{x}_{ai} - P_j r_j. \tag{7.45}$$

7.3.3   Static Properties of the Min–Max Arrangement with State Feedback

The static analysis conducted for the min–max arrangement with dynamic compensators is repeated for the state feedback case. The same fundamental issues are discussed: determining the regulator that becomes active at the initial time ($t = 0$), determining the regulator that remains active during a steady-state regime ($t \to \infty$), and establishing conditions for limits to be preserved at steady-state. Unlike min–max systems with control transfer functions, initial conditions have an effect in the initial regulator selection. Since linear systems are considered, initial conditions do not determine steady-state properties, however.

7.3.3.1   Initial Regulator: Min-Only Case

Using (7.45) directly, the initial regulator i_0 must satisfy

$$(K_j - K_{i_0})\tilde{x}_{ai_0}(0) \leq -K_j\bar{x}_{ai_0} + P_j r_j$$

for all $j \in L$. Using identity (7.34), i_0 is determined as the smallest index satisfying

$$(K_j - K_{i_0})\tilde{x}_{ai_0}(0) \leq -M_j \frac{r_{i_0}}{G_{i_0}(0)} + P_j r_j \tag{7.46}$$

for all $j \in L$ where the scalar M_j is defined as

$$M_j = K_j \begin{bmatrix} -A^{-1} & B \\ & 1 \end{bmatrix}. \tag{7.47}$$

7.3.3.2   Initial Regulator: Max-Only Case

Simply reversing inequality (7.46), we see that initial regulator i_0 is the smallest index satisfying

$$(K_j - K_{i_0})\tilde{x}_{ai_0}(0) \geq -M_j \frac{r_{i_0}}{G_{i_0}(0)} + P_j r_j \tag{7.48}$$

for all $j \in H$.

7.3.3.3 Initial Regulator: Min–Max Case

The logic is the same as for the dynamic compensator case: if $i_0 \in L$, the following inequalities must hold:

$$(K_j - K_{i_0})\tilde{x}_{ai_0}(0) \leq -K_j \bar{x}_{a_{i_0}} + P_j r_j \text{ for all } j \in L, \tag{7.49}$$

$$(K_j - K_{i_0})\tilde{x}_{ai_0}(0) \geq -M_k \frac{r_{i_0}}{G_{i_0}(0)} + P_k r_k \text{ for all } k \in H. \tag{7.50}$$

If $i_0 \in H$, however, the following inequalities apply:

$$(K_j - K_{i_0})\tilde{x}_{ai_0}(0) \geq -M_k \frac{r_{i_0}}{G_{i_0}(0)} + P_k r_k \text{ for all } k \in H, \tag{7.51}$$

$$(K_j - K_{i_0})\tilde{x}_{ai_0}(0) > \min_{j \in L} \{u_{rj}(0)\}. \tag{7.52}$$

A guess must be made regarding whether $i_0 \in L$ or $i_0 \in H$ and the corresponding inequalities verified.

7.3.3.4 Steady Regulator: Min-Only Case

Suppose i^* is the index of the steady regulator. Then $\dot{u} = u_{ri^*} = 0$ and $\tilde{x}_{ai^*} = 0$. Equation (7.45) is used directly to determine that i^* is the smallest index satisfying

$$M_j \frac{r_{i^*}}{G_{i^*}(0)} \leq P_j r_j$$

for all $j \in L$. If P_j is designed so that $y_j = r_j$ in steady-state (i.e., according to (7.35)), then the reader can verify that i^* is the smallest index satisfying

$$\frac{1}{G_j(0)} M_j \left(\bar{y}_{j/i^*} - r_j\right) \leq 0, \tag{7.53}$$

where $\bar{y}_{j/i^*} = G_j(0) r_{i^*}/G_{i^*}(0)$ is the steady value attained by y_j when i^* is active at steady state. This result is interpreted in a similar way as done for the dynamic compensator case, where $M_j/G_j(0)$ plays the role of the compensator's low-frequency gain $K(0)$: when $M_j/G_j(0) > 0$, i^* is the regulator for which outputs do not exceed their setpoints at steady-state. If $M_j/G_j(0) < 0$, i^* is the regulator for which outputs do not become smaller than their setpoints at steady-state. Note from (7.35) that $M_j/G_j(0) \neq 0$, otherwise the tracking task would not be possible.

7.3.3.5   Steady Regulator: Max-Only Case

In this case, i^* is the smallest index satisfying

$$\frac{1}{G_j(0)} M_j \left(\bar{y}_{j/i^*} - r_j \right) \geq 0 \tag{7.54}$$

for all $j \in H$. When $M_j/G_j(0) > 0$, i^* is the regulator for which outputs do not become smaller than their setpoints at steady-state. When $M_j/G_j(0) < 0$, i^* is the regulator for which outputs do not exceed their setpoints at steady-state.

In summary, when $M_j/G_j(0) > 0$, the min selector protects upper-limited outputs at steady-state and the max selector protects lower-limited outputs at steady-state. When $M_j/G_j(0) < 0$, the reverse steady-state protections are afforded.

7.3.3.6   Steady Regulator: Min–Max Case

If $i^* \in L$, the following inequalities must hold:

$$M_j \frac{r_{i^*}}{G_{i^*}(0)} \leq P_j r_j, \tag{7.55}$$

$$M_k \frac{r_{i^*}}{G_{i^*}(0)} \geq P_k r_k \tag{7.56}$$

for all $j \in L$ and all $k \in H$. If there exist values of j or k for which the above inequalities fail, then it must be that $i^* \in H$ and the following inequalities must hold:

$$M_k \frac{r_{i^*}}{G_{i^*}(0)} \geq P_k r_k, \tag{7.57}$$

$$\min \left\{ -M_j \frac{r_{i^*}}{G_{i^*}(0)} + P_j r_j \right\} < 0 \tag{7.58}$$

for all $k \in H$, with the minimum in inequality (7.58) is taken over $j \in L$. These conditions can be interpreted following a similar process as done for the isolated min and max cases. Suppose first that $i^* \in L$. Inequalities (7.55) and (7.56) can be written as

$$\frac{M_j}{G_j(0)} (\bar{y}_{j/i^*} - r_j) \leq 0, \tag{7.59}$$

$$\frac{M_k}{G_k(0)} (\bar{y}_{k/i^*} - r_k) \geq 0 \tag{7.60}$$

Table 7.1 Guidelines for the association of outputs to selectors based on steady-state characteristics. When using the min–max arrangement, $i^* \in L$ is required

Case	Sign of $M_j/G_j(0)$	Association
I: All upper-limited,	+	Min only
$\text{sign}\left(\frac{M_j}{G_j(0)}\right)$ constant	–	Max only
II: All lower-limited,	+	Max only
$\text{sign}\left(\frac{M_j}{G_j(0)}\right)$ constant	–	Min only
III: All upper-limited,	+	Min in min–max
mixed $\text{sign}\left(\frac{M_j}{G_j(0)}\right)$	–	Max in min–max
IV: All lower-limited,	+	Max in min–max
mixed $\text{sign}\left(\frac{M_j}{G_j(0)}\right)$	–	Min in min–max
Mixed limits,		Use min–max
V: mixed $\text{sign}\left(\frac{M_j}{G_j(0)}\right)$		As in III and IV

for all $j \in L$ and all $k \in H$. Thus, min-linked outputs y_j such that $M_j/G_j(0) > 0$ and max-linked y_k outputs such that $M_k/G_k(0) < 0$ will remain below their setpoints at steady-state. Similarly, min-linked outputs y_j such that $M_j/G_j(0) < 0$ and max-linked y_k outputs such that $M_k/G_k(0) > 0$ will remain above their setpoints at steady-state. Now suppose design parameters are chosen so that $i^* \in H$. Inequality (7.60) holds for all $k \in H$, but min-linked outputs must satisfy the following:

$$0 > \min\left\{\frac{M_j}{G_j(0)}(r_j - \bar{y}_{j/i^*})\right\}.$$

When $M_j/G_j(0) < 0$ we have

$$\min\left\{\frac{M_j}{G_j(0)}(r_j - \bar{y}_{j/i^*})\right\} = \frac{M_j}{G_j(0)}\max\left\{r_j - \bar{y}_{j/i^*}\right\}.$$

It follows that $r_j < \bar{y}j/i^*$ for all $j \in L$, indicating that min-linked variables are lower-limited by r_j, matching the min-only result. However, if $M_j/G_j(0) > 0$, we can only say:

$$0 > \min\left\{r_j - \bar{y}_{j/i^*}\right\}$$

and no bounds can be guaranteed for $\bar{y}_{j/i^*}$. Thus, if the design requires $i^* \in H$ for some reason, only lower-limited outputs having $M_j/G_j(0) < 0$ should be linked to the min-selector.

The preceding analysis can be regarded as a design guideline for the association of outputs to selectors. This is done solely on the basis of steady-state characteristics. The guidelines have been summarized in Table 7.1.

7.3.4   Example: CMAPSS-1 Linearized Model

Consider the same transfer functions of Example 7.1.3. Matrices A and B of the state-space realization are as follows:

$$A = \begin{bmatrix} -3.8420 & 1.4125 \\ 0.5310 & -4.6623 \end{bmatrix}, \quad B = \begin{bmatrix} 230.9226 \\ 653.7255 \end{bmatrix}.$$

For $y_1 = \Delta N_f$, $C_1 = [1 \ 0]$ and $D_1 = 0$. The values of matrices C and D for ΔT_{48} are $C = [-0.1022 \ -0.2952]$ and $D = 146.24$. Finally, a state-space realization of the transfer function to $\Delta SmHPC$ using the same A and B has $C = [0.0189 \ 0.0066]$ and $D = -4.4052$. Note that this flight condition is close, but not equal to FC01 listed in Appendix B

Consider first that y_1 must be driven to a setpoint $r_1 = 100$ rpm while preventing $y_2 = \Delta T_{48}$ from exceeding $r_2 = 200°R$. That is, y_2 is an upper-limited output. The individual regulators are designed using an LQR approach for the augmented plant, with $Q = C_{a1}^T C_{a1}$ and $Q = C_{a2}^T C_{a2}$, where $C_{a1} = [C_1 \ D_1]$ and $C_{a2} = [C_2 \ D_2]$ are the augmented output matrices. Using $R = 1$ for both designs, the resulting state-feedback gains are

$$K_1 = [0.7098 \ 0.0840 \ 20.9204],$$
$$K_2 = [-0.1006 \ -0.2870 \ 144.7929].$$

The required values of P_1 and P_2 for perfect tracking when the regulators are used independently are $P_1 = 1$ and $P_2 = 1$, with $\bar{x}_{a1}^T = [100 \ 131.7106 \ 0.8581]$, as determined from formulas (7.35) and (7.34). Suppose that a min selector is used and, for illustrative purposes, that the input integrator has initial condition $u(0) = 1$. Then $\tilde{x}_{a1}(0) = [-100 \ -131.7106 \ 0.1419]$. The initial regulator is then $i_0 = 2$ by application of condition (7.46). Similarly, condition (7.53) predicts that $i^* = 1$. This is confirmed by the simulation results of Fig. 7.5. If the min selector is not used and a feedback loop is established to control y_1 to its setpoint, y_1 has a settling time of about 0.4 s and zero steady-state error by design. Output y_2, however, exceeds its intended limit by far during the transient regime and settles at $\bar{y}_{2/1} = 76.39 < r_2$. If the min selector is used, u_{r2} is active from $t = 0$ until $t = 0.22$, which causes y_2 to be regulated toward its limit. A regulator switching occurs near $t = 0.22$ and $i = 1$ becomes active for all subsequent times. Note that y_1 overshoots its limit by about 2%. Thus, this example shows that the min selector preserved limits during the transient regime for y_2 but not for y_1, motivating further analysis of limit protection properties. This is done in Sect. 7.3.5. Now suppose ΔT_{48} is not a concern, but that the HPC stall margin must be kept above certain limit to minimize the risk of stall or surge. Define $y_2 = \Delta SmHPC$ and suppose that the stall margin must not decrease more than 10% from its steady value at FC01, that is y_2 must be lower-limited by $r_2 = -10$. References to the standard min–max arrangement used in the GTE
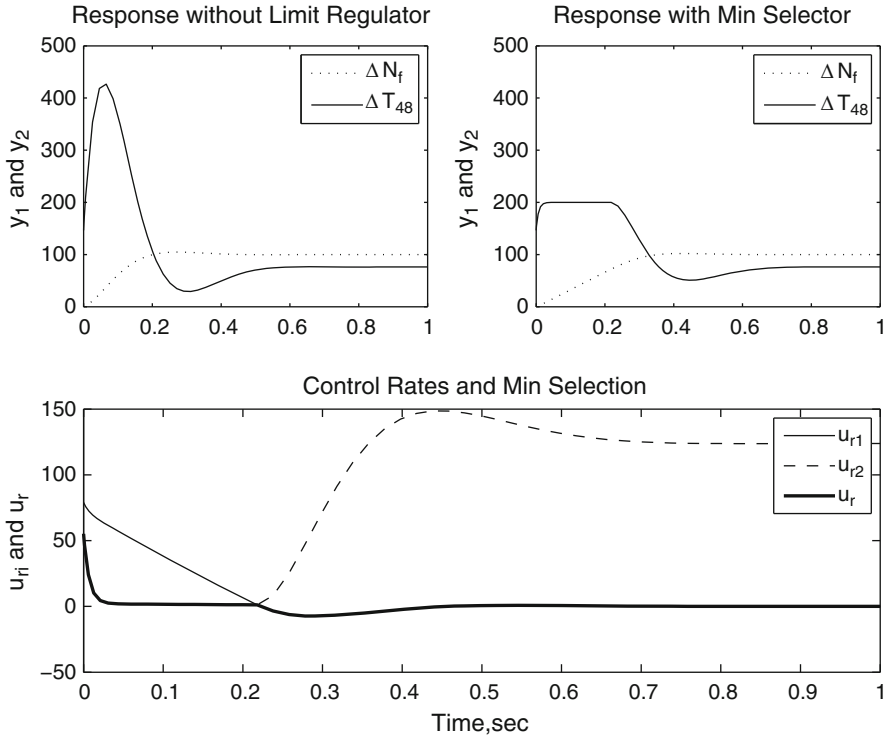
Fig. 7.5 Response of state-feedback system with min selector: CMAPSS-1 linearized model with upper-limited output $y_2 = \Delta T_{48}$

industry assume a priori that the regulators of lower-limited outputs are applied to the ports of a max selector. As this example demonstrates, the choice of selector must take additional considerations into account. Suppose K_2 is designed using an LQR approach with $Q = C_{a2}^T C_{a2}$ and $R = 1$, and K_1 and r_1 are maintained. Now,

$$K_2 = [-0.0097 \quad -0.0045 \quad 3.0135]$$

and $P_2 = -1$. If, according to conventional wisdom, the max selector is used, it can be verified that $i_0 = 1$ and $i^* = 2$. As shown in Fig. 7.6, the results are disastrous. Since $i^* = 2$, the lower limit imposed on y_2 is preserved at steady-state, but $\bar{y}_{1/2} = 975.98$, far above r_1. Also, y_2 becomes smaller than its limit during the transient. If a min selector is used instead, the results are acceptable if fan speed is allowed to overshoot. In this case, $i_0 = 2$ and $i^* = 1$. Since $\bar{y}_{2/1} = -1.02$, the lower limit imposed in y_2 is still preserved at steady-state, and moreover, transient limit protection is observed. To illustrate the initial and steady properties of the min–max arrangement, consider the following output definitions: $y_1 = \Delta N_f$, $y_2 = \Delta T_{48}$, $y_3 = \Delta \text{Ps30}$ and $y_4 = \Delta(W_F/\text{Ps30})$. The last two outputs are the incremental
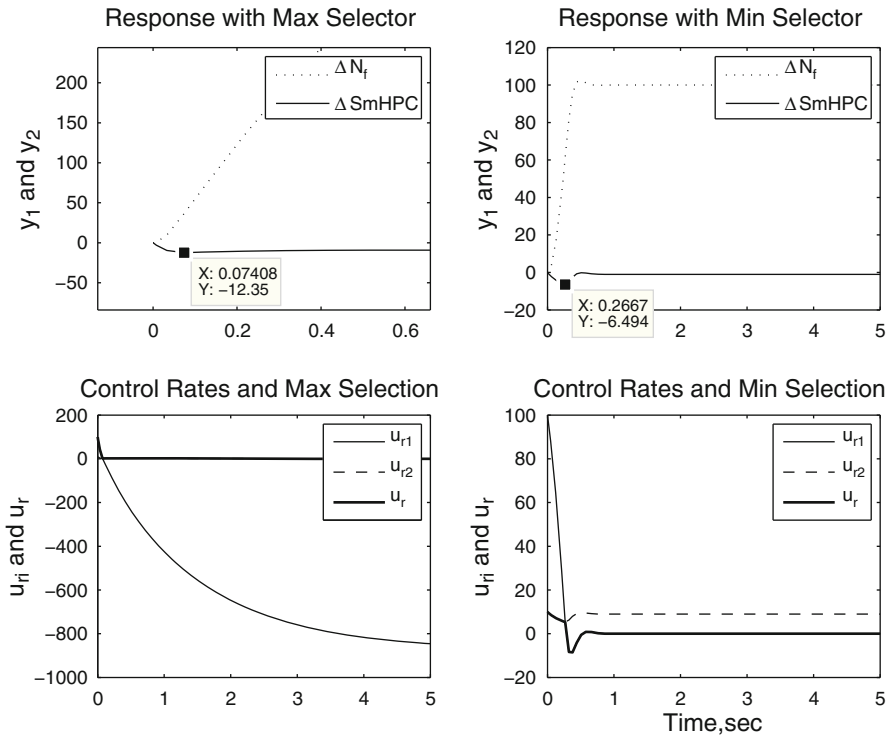
Fig. 7.6 Response of state-feedback system with max and min selectors: CMAPSS-1 linearized model with lower-limited output $y_2 = \Delta$ SmHPC

static pressure at HPC outlet, and the incremental ratio between fuel flow and Ps30. To prevent lean blowout conditions in the combustor, y_3 is lower-limited. A low limit is usually imposed on y_4 to prevent the LPC from stalling.

The linearized C and D parameters for y_3 and y_4 can be found in Appendix B. The state feedback gains are designed using an LQR approach with $Q = C_{ai}^T C_{ai}$ and $R = 1$ as before. The resulting gains are

$$K_3 = [0.0639 \ 0.1534 \ 25.2464],$$

$$K_4 = [-0.0039 \ -0.0085 \ 3.5781]$$

with corresponding values of $P_3 = 1$ and $P_4 = 1$. The two upper-limited outputs are linked to the min selector, while the lower-limited outputs are linked to the max selector. Consider setpoints as follows: $r_1 = 100$, $r_2 = 200$, $r_3 = -50$, and $r_4 = -20$. Formulas (7.49)–(7.52) can be used to determine that $i_0 = 1$. Likewise, formulas (7.55)–(7.58) indicate that $i^* = 1$. The response to this case is shown in Fig. 7.7. Since y_3 and y_4 have DC gains $G_3(0) = G_4(0)$ with the same sign as $G_1(0)$, their DC value increases when $r_1 > 0$. Therefore, they move away from their
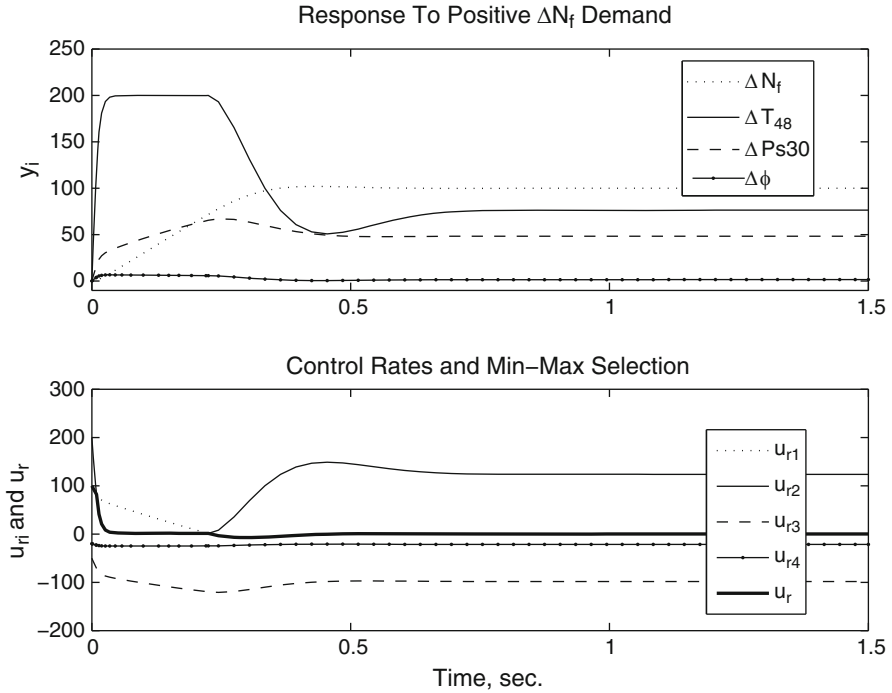
Fig. 7.7 Response of state-feedback system with min–max selectors: CMAPSS-1 linearized model with upper-limited output $y_2 = \Delta T_{48}$ and lower-limited outputs $y_3 = \Delta Ps30$ and $y_4 = \Delta W_F/Ps30$ (fan speed increase demand)

negative limits and their regulators are never active. As in the previous example, the T_{48} limit regulator becomes active in the transient regime. Now suppose $r_1 = -100$ rpm. In this case, y_3 and y_4 decrease from their initial values. It can be verified that $i_0 = 4$ and $i^* = 1$. As shown in Fig. 7.8, the 4th regulator remains active for some time after $t = 0$ and y_3 and y_4 are maintained above their lower limits at steady state, as well as during the transient.

7.3.5 Transient Limit Protection Analysis

The invariance condition for intervals presented in Sect. 7.2.1 is now applied to study the limit protection properties of the min–max approaches with static state feedback. Analysis is divided into three cases corresponding to min-only, max-only, and min–max selectors. For upper-limited outputs, the error $e = r - y$ must not become negative. That is, $[0, \infty)$ must be positively invariant. For lower-limited outputs, e must not become positive, that is, $(-\infty, 0]$ must be positively invariant.
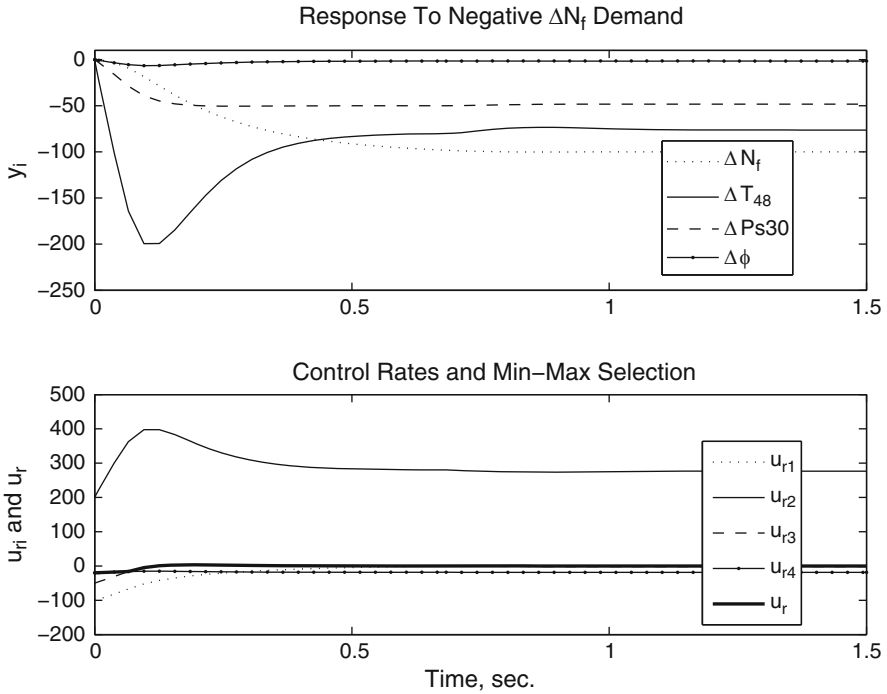
Fig. 7.8 Response of state-feedback system with min–max selectors: CMAPSS-1 linearized model with upper-limited output $y_2 = \Delta T_{48}$ and lower-limited outputs $y_3 = \Delta Ps30$ and $y_4 = \Delta W_F/Ps30$ (fan speed decrease demand)

The sign of $\dot{e}$ must be examined along the boundary $e = 0$ to determine invariance. Given a fixed i and $j \neq i$, five sets are relevant:

1. $\mathcal{U}_{ij}$: the set where $u_{ri} = u_{rj}$
2. $\mathcal{E}_i$: the set where $e_i = 0$
3. $\mathcal{E}_j$: the set where $e_j = 0$
4. $\dot{\mathcal{E}}_i$: the set where $\dot{e}_{i/i} = 0$
5. $\dot{\mathcal{E}}_{j/i}$: the set where $\dot{e}_{j/i} = 0$

Set $\mathcal{U}_{ij}$ represents the boundary between the two half-spaces which are the regions of activity of each regulator, and the roles of the other sets are clear from their definitions. For the min-only or max-only cases, the sets are hyperplanes, as represented in Figs. 7.9 and 7.10. Sets $\dot{\mathcal{E}}_i$ and $\dot{\mathcal{E}}_{j/i}$ divide the space into two halves, one where the error increases and the other where the error decreases, and this has been indicated with plus or minus signs.

For upper-limited variables, the invariance condition requires that the derivative of the error be nonnegative whenever the error is zero. Now, as seen in Figs. 7.9 and 7.10, $\mathcal{E}_i$ and $\mathcal{E}_{j/i}$ are divided into two regions, corresponding to positive and

Fig. 7.9 Schematic of the regions corresponding to sets $\mathcal{U}_{ij}$, $\mathcal{E}_i$ and $\dot{\mathcal{E}}_i$
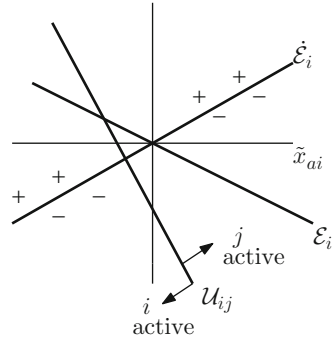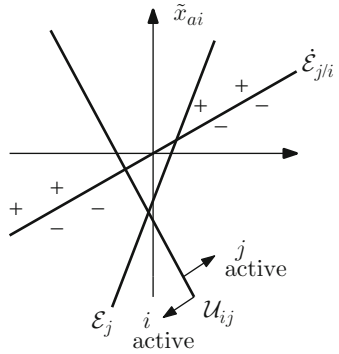

Fig. 7.10 Schematic of the regions corresponding to sets $\mathcal{U}_{ij}$, $\mathcal{E}_j$ and $\dot{\mathcal{E}}_{j/i}$

negative error derivatives. Assuming that i is the active regulator, *limit protection is ensured by requiring that the regions of $\mathcal{E}_i$ and $\mathcal{E}_{j/i}$ where, the error increases lie outside the region where i is active.* That is, the intersection of $\dot{\mathcal{E}}_i$ and $\mathcal{E}_i$ must be outside the half space where i is active, and the intersection of $\dot{\mathcal{E}}_{j/i}$ and $\mathcal{E}_j$ must likewise be outside the half space where i is active.

Equations (7.39) and (7.43) are combined to determine the set $\dot{\mathcal{E}}_i \cap \mathcal{E}_i$, resulting in the following system of linear equations on $\tilde{x}_{ai}$:

$$\begin{bmatrix} -C_{ai} \\ -C_{ai} A_{ci} \end{bmatrix} \tilde{x}_{ai} = \begin{bmatrix} 0 \\ 0 \end{bmatrix}. \tag{7.61}$$

The matrix characterizing the above system of equations is full-rank, unless C_{ai} and $C_{ai} A_{ci}$ are parallel vectors. For this to happen, there would have to exist a scalar λ such that $C_{ai} A_{ci} = \lambda C_{ai}$. Taking the transpose of this equation, we get

$$A_{ci}^{\mathrm{T}} C_{ai}^{\mathrm{T}} = \lambda C_{ai}^{\mathrm{T}}$$

that is, C_{ai}^{T} would have to be an eigenvector of A_{ci}^{T}. Assuming that K_i has been verified not to produce this exception, the only solution to system (7.61) is $\tilde{x}_{ai} = 0$.

Likewise, (7.40) and (7.44) are combined to determine the set $\dot{\mathcal{E}}_{j/i} \cap \mathcal{E}_j$, resulting in the following system of linear equations on $\tilde{x}_{ai}$:

$$\begin{bmatrix} -C_{aj} \\ -C_{aj} A_{ci} \end{bmatrix} \tilde{x}_{ai} = \begin{bmatrix} \bar{e}_{j/i} \\ 0 \end{bmatrix}. \tag{7.62}$$

System (7.62) does not have a unique solution in general. In this case, it becomes necessary to find particular ones that assist in arriving at invariance conditions. This is done separately for the min-only, max-only, and min–max cases.

7.3.5.1   Transient Limit Protection: Min-Only Case

Suppose all variables are upper-limited. To guarantee that y_i will not exceed its upper limit, we require that $u_{ri} - u_{rj} > 0$ along solutions to (7.61). If C_{ai}^{T} is not an eigenvector of A_{ci}^{T}, $\tilde{x}_{ai} = 0$ is the only solution. Using (7.45), we see that the required inequality reduces to $K_j \bar{x}_{ai} > P_j r_j$ for all $j \in L$. Using (7.34) and the definition of M_j from (7.47), this becomes:

$$M_j \frac{r_i}{G_i(0)} > P_j r_j \tag{7.63}$$

for all $j \in L$. Noting that inequality (7.63) is the opposite of inequality (7.53), we see that transient limit protection cannot be guaranteed for $i = i^*$, even for intervals of time where i^* is active! This can be confirmed in the min-only case of Example 7.3.4, where $i^* = 1$ and y_1 exhibits overshoot while its own regulator is active. In the max-only case where $i^* = 2$, y_2 violates its limit in the transient regime, even when its regulator is active. These shortcomings are removed by using sliding mode controllers instead of linear regulators (See Chap. 8).

Now consider the condition for y_j not to exceed its upper limit while i is active. For this, we require that $u_{ri} - u_{rj} > 0$ along solutions to (7.62). Since there is no explicit solution in this case, the solution that minimizes $u_{ri} - u_{rj}$ is sought, followed by a requirement that the minimum solution be positive. Mathematically, the invariance condition can be expressed as

$$(K_j - K_i)\tilde{x}_{ai}^* > -K_j \bar{x}_{ai} + P_j r_j,$$

where $\tilde{x}_{ai}^*$ is the solution to the following constrained minimization problem:

$$\tilde{x}_{ai}^* = \arg \min (K_j - K_i)\tilde{x}_{ai}$$

$$\text{subject to}$$

$$\begin{bmatrix} -C_{aj} \\ -C_{aj} A_{ci} \end{bmatrix} \tilde{x}_{ai} = \begin{bmatrix} \bar{e}_{j/i} \\ 0 \end{bmatrix}. \tag{7.64}$$

A negative test for invariance can be conducted by finding *any* solution to system (7.62) and checking whether $u_{ri} \leq u_{rj}$ is satisfied for all $j \in L$ for that particular value of $\tilde{x}_{ai}$. If so, the set $\dot{\mathcal{E}}_{j/i} \cap \mathcal{E}_j$ contains at least one point for which the active regulator is i and invariance for y_j cannot be concluded.

7.3.5.2   Transient Limit Protection: Max-Only Case

The corresponding invariance conditions for y_i and y_j are obtained by reversing the inequalities in (7.63) and (7.64), and are the same whether upper- or lower-limited variables are involved. That is, invariance for y_i is guaranteed if:

$$K_j \bar{x}_{ai} < P_j r_j \tag{7.65}$$

for all $j \in H$. Similarly, invariance for y_j is guaranteed if:

$$(K_j - K_i)\tilde{x}_{ai}^* < -K_j \bar{x}_{ai} + P_j r_j,$$

where $\tilde{x}_{ai}^*$ is the solution to the following constrained minimization problem:

$$\tilde{x}_{ai}^* = \arg\min (K_j - K_i)\tilde{x}_{ai}$$

$$\text{subject to}$$

$$\begin{bmatrix} -C_{aj} \\ -C_{aj} A_{ci} \end{bmatrix} \tilde{x}_{ai} = \begin{bmatrix} \bar{e}_{j/i} \\ 0 \end{bmatrix}. \tag{7.66}$$

Although the invariance conditions for the min-only and max-only cases were developed used two regulators, their validity extends to more than two regulators by considering all possible pairs of regulators.

7.3.5.3   Transient Limit Protection: Min–Max Case

In this case, analysis must be made in groups of three regulators, an arbitrary fixed regulator i assumed active, a regulator j in the min group, and a regulator k in the max group. Two cases must be considered: $i \in L$ and $i \in H$. Assuming $i \in L$, the region where i is active is given by $\mathcal{U}_L \cap \mathcal{U}_H$, where:

$$\mathcal{U}_L = \{\tilde{x}_{ai} \; : \; u_{ri} - u_{rj} \leq 0 \text{ for all } j \in L\},$$

$$\mathcal{U}_H = \{\tilde{x}_{ai} \; : \; u_{ri} - u_{rk} \geq 0 \text{ for all } k \in H\}.$$

Invariance will be guaranteed if $\dot{\mathcal{E}}_i \cap \mathcal{E}_i$ lies outside $\mathcal{U}_L \cap \mathcal{U}_H$. As before, if $\tilde{x}_{ai} = 0$ is the only element of $\dot{\mathcal{E}}_i \cap \mathcal{E}_i$, the invariance conditions reduce to

$$K_j \bar{x}_{ai} > P_j r_j, \tag{7.67}$$

$$K_k \bar{x}_{ai} < P_k r_k \tag{7.68}$$

for all $j \in L$ and for all k in H. For a regulator $i \in H$, the region where it is active is given by $\mathcal{U}_H \cap \mathcal{U}_l$, where $\mathcal{U}_l$ is defined as

$$\mathcal{U}_l = \left\{ \tilde{x}_{ai} \ : \ u_{ri} > \ \min \ \{u_{rj}\}, j \in L \right\}.$$

The reader will observe that this set has a complex description. Establishing the invariance of y_j while i is active is also rather difficult. First, j must be assumed to begin to either L or H. For each case, subcases corresponding to $i \in L$ and $i \in H$ must be contemplated. This process is best handled numerically, with the aid of a computer program.

7.4   Example: CMAPSS-1 Linearized Model

Continuing with Example 7.3.4, consider first the problem of establishing transient limit protection when only the min selector is used. It can be verified that C_{a1} is not parallel to $C_{a1} A_{ci}$ and therefore $\tilde{x}_{a1} = 0$ is the only solution to system (7.61). Thus, no transient limit protection can be guaranteed for i^*. Although (7.63) is only a sufficient condition, simulation showed that y_1 overshoots its limit in the transient regime, even for intervals when its own regulator is active. To see whether invariance can be established for y_2 while $i^* = 1$ is active, note that $\bar{y}_{2/1} = 76.39$, so $\bar{e}_{2/1} = 123.61$. An exact solution to system (7.62) can be readily found using the pseudoinverse as $\tilde{x}_{a1}^T = [25.4488 \quad 4.2484 \quad -0.8189]$. Evaluating $u_{r1} - u_{r2}$ at this value using (7.45) gives -247.25, indicating, again, that there is a point where $e_2 = \dot{e}_{2/1} = 0$ with $i = 1$ being active. Therefore, invariance for y_2 cannot be concluded during the transient regime for periods where $i = 1$ is active. Simulation shows, however, that y_2 remains below its limit. The conservativeness of the sufficient condition can be traced to the fact that the solution found for $\tilde{x}_{a1}$ does not belong to the actual state trajectory followed by the system. A refined version of the invariance condition would require taking into account such trajectories, which depend on the previous switching history.

Now consider the max-only case of Example 7.3.4. Again, no transient limit protection can be guaranteed for $i^* = 2$ for periods where this regulator is active. Condition (7.63), is satisfied for $i = 1$, however. Therefore, y_1 will not exceed its limit when its own regulator is active. In this example $i_0 = 1$, and $i = 1$ remains active for a short time, where $y_1 < r_1$, verifying transient invariance for this case.

A regulator switching occurs and the active regulator becomes $i^* = 2$ for all future times. Invariance cannot be concluded for y_2 while $i = 2$ is active, and simulation confirms that y_2 becomes smaller than its limit.

The preceding steady and transient limit protection analysis, as well as the examples, suggest that the standard min–max arrangement may be ill-conceived, at least when used in conjunction with linear regulators. Although steady limit preservation is achieved in a simple fashion, there is no clear way to guarantee that outputs will remain within their prescribed bounds in the transient regime. When sliding mode controllers are used, stability and limit protection are guaranteed under most cases, as described in Chap. 8.

7.5 Alternative Minimum-Interaction Design: $\mathcal{H}_\infty$ Approach

A reasonable alternative to using limit regulators is to design the state feedback gain so that one of the outputs (say, fan speed) has a suitably fast transient response while the other outputs are suppressed during transients, minimizing the possibility of limit violations. This problem can be formulated using the multiobjective $\mathcal{H}_\infty$ state feedback synthesis discussed in Chap. 4. Adequate fan speed response is obtained by the built-in robust stability property, together with a regional eigenvalue placement constraint. Limited outputs are regarded as performance outputs z_2 or z_∞. The latter choice is convenient when output disturbances are included, since the $\mathcal{H}_\infty$ norm remains finite even for nonstrictly proper transfer functions.

7.5.1 Example: CMAPSS-1

The constant feedback gain $\mathcal{H}_\infty$ design is now applied to the fan speed control problem near FC01. System parameters are given in Appendix B. Recalling the developments of Chap. 4, the robust state feedback synthesis approach handles the system description given below:

$$\dot{x}_a = A_a x_a + B_a u_r + \Gamma_a w, \tag{7.69}$$

$$z_\infty = C x_a, \tag{7.70}$$

where w is a vector of disturbances. Matrix Γ has not been listed in Appendix B, but may be obtained through linearization using the CMAPSS-1 interface. The objective is to find a feedback gain K stabilizing the augmented closed-loop matrix $A_c = A_a - B_a K$ while minimizing the infinity norm of the transfer function from w to z_∞. The designer controls fan speed response by specifying a target region for the closed-loop eigenvalues of A_c. The $\mathcal{H}_\infty$ minimization objective translates into transient suppression of the limited outputs. The presence of a disturbance
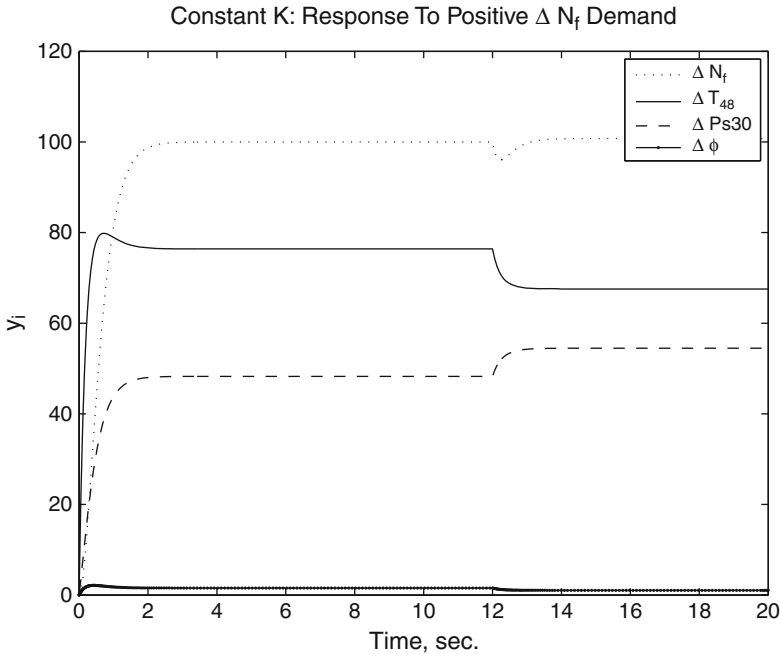
Fig. 7.11 Response of limited outputs for minimum interaction design: positive ΔN_f demand

component introduces a design tradeoff. The larger the influence of disturbances (as measured through matrix Γ), the smaller the closed-loop allowable bandwidth. This can be observed when carrying the design using, for instance, the `msfsyn` command: Γ may need to be scaled to maintain feasibility.

In this example, Γ is scaled to 10% of their linearization value. A disk centered at -10 with radius 7 is used as the target region, resulting in an $\mathcal{H}_\infty$ norm of 169 and a feedback gain as follows:

$$K = [0.0001 \quad -0.0008 \quad 3.8233],$$

which places the closed-loop eigenvalues of A_c at -5.444, -3.8419, and -3.0417. Using a fan speed demand of $\Delta N_f = 100$ rpm, it can be verified that the corresponding steady values of the limited outputs are $\Delta T_{48} = 75.835°$ R, Δ Ps30=48.26 psi and $\Delta \Phi = 1.56$ pps/psi. As Fig. 7.11 shows, the transient peak of ΔT_{48} remains under the limit of $r_2 = 200$ that was used in the previous examples. A step health parameter disturbance was applied at $t = 12$ s. Figure 7.12 corresponds to $\Delta N_f = -100$ rpm. In this case, all limited outputs remain within the bounds used in the previous examples.
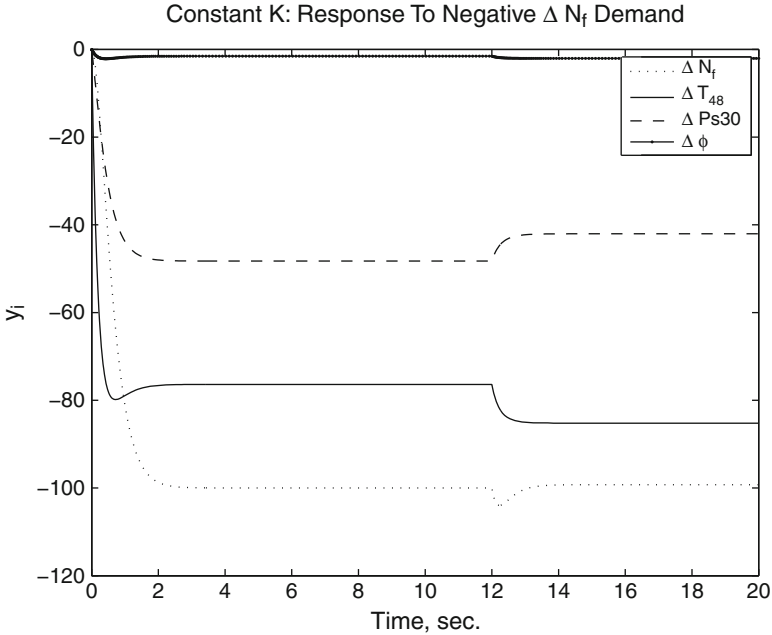
Constant K: Response To Negative ΔN_f Demand

Fig. 7.12 Response of limited outputs for minimum interaction design: negative ΔN_f demand

7.5.2 Example: Ellipsoidal Invariant Set: CMAPSS-1 Linearized Model

An ellipsoidal invariant set is now derived for the closed-loop system of the previous example, first using the feedback gain obtained through $\mathcal{H}_\infty$ synthesis. Define a shifted state vector as done in Sect. 7.3.2:

$$\tilde{x}_a = x_a - \bar{x}_a,$$

where $\bar{x}_a$ represents a target state so that $y_1 = r_1$ when the system reaches steady-state. The state-feedback law for fan speed setpoint tracking is $u_r = -Kx_a + Pr_1$, which can be written in terms of $\tilde{x}_a$ as follows:

$$u_r = -Kx_a + Pr_1 = -K(\tilde{x}_a - \bar{x}_a) + Pr_1 = -K\tilde{x}_a,$$

where (7.33) has been used. Recalling that $A_a\bar{x}_a = 0$, substitution of the above control law into system (7.69) yields the following closed-loop dynamics

$$\dot{\tilde{x}}_a = (A_a - B_aK)\tilde{x}_a.$$

Now, the constraints are formulated in terms of x_a from the limited output specifications:

$$y_2 = C_{a2}\tilde{x}_a \leq r_2,$$
$$y_3 = C_{a3}\tilde{x}_a \geq r_3,$$
$$y_4 = C_{a3}\tilde{x}_a \geq r_4.$$

Note that the first output (incremental fan speed) has not been regarded as a limited output, but if necessary, it can be directly added to the list of constraints. The constraint vectors are now normalized so that they correspond to the assumed description $G_i x \leq 1$. For this, inequalities reflecting positive upper bounds are simply divided by the value of the bound. For negative lower bounds, the left-hand and right-hand sides of the inequality are switched and the inequality divided by the negative of the bound. According to this, the three constraints adopt the desired form, with $G_2 = C_{a2}/r_2$, $G_3 = C_{a3}/r_3$, and $G_4 = C_{a4}/r_4$.

An arbitrary symmetric, positive-definite matrix Q may be used to obtain a family of invariant ellipsoids from the solution of Lyapunov equation (7.24). For each constraint, the largest admissible ellipsoid from this family is found by calculating its V_i value. The smallest V_i, say V, is then selected, and the operating set for $\tilde{x}_a$ is defined as $\tilde{x}_a^T P \tilde{x}_a \leq V$. Although this guarantees invariance, the orientation of the ellipsoid may not be the best for the given constraints. An improvement is to find P to maximize the volume of the ellipsoid, subject to the invariance condition (7.23) and $G_i \tilde{x}_a \leq 1$, see O'Dell [62].

As an example, take $Q = I$. The Lyapunov equation is solved using `lyap((Aa-Ba*K)',Q)` to yield

$$P = \begin{bmatrix} 0.1342 & 0.0303 & 7.3913 \\ 0.0303 & 0.1184 & 11.4089 \\ 7.3913 & 11.4089 & 2397.3 \end{bmatrix}.$$

The values of V_i are calculated as $V_2 = 1438.7$, $V_3 = 8780.9$, and $V_4 = 9526.1$. Therefore, the operating set for $\tilde{x}_a$ is described by the inequality $\tilde{x}_a^T P \tilde{x}_a \leq 1438.7$.

This result can be given a practical interpretation by considering the meaning of $\tilde{x}_a$. The operating set restricts the distance between $x_a(0)$ and $\bar{x}_a$, the target state. Recalling that $x_a^T = [\Delta N_f \ \Delta N_c \ \Delta W_F]$ is the incremental state relative to a steady linearization point, we see that $x_a(0) = 0$ if the setpoint change maneuver starts at the linearization point. For such cases, we can restrict the target state to guarantee limit protection by enforcing $\bar{x}_a^T P \bar{x}_a \leq 11.3$. Using (7.34), this inequality becomes

$$\left(\frac{r_1}{G_1(0)}\right)^2 \begin{bmatrix} -A^{-1}B \\ 1 \end{bmatrix}^T P \begin{bmatrix} -A^{-1}B \\ 1 \end{bmatrix} \leq 1,$$

which in this example reduces to $|r_1| \leq 38.3$, a conservative figure. Now consider the problem of finding a stabilizing K that maximizes the volume of an invariant ellipsoid contained in the constrained set. This problem can be solved using O'Dell's techniques [62], yielding the following combination of P and K:

$$P = \begin{bmatrix} 0.00000219 & 0.00000537 & 0.00064 \\ 0.00000537 & 0.00001354 & 0.00121 \\ 0.00064366 & 0.00121329 & 1.12223 \end{bmatrix},$$

$$K = [0.000578 \ 0.001120 \ 0.877210].$$

This feedback gain places the closed-loop eigenvalues at -1.251, -2.965, and -5.165, producing a somewhat slower response in comparison with the value obtained through $\mathcal{H}_\infty$ synthesis. The minimum value of V is now 1 and the bound for r_1 becomes 78.8 rpm, a less conservative value. This value is still far from the maximum value of r_1 for which a limited output reaches its limit. Indeed, since all closed-loop poles are real, no output will exhibit overshoot. Thus, an upper-limited variable y_j can only reach r_j in the steady state. For this, r_{i*} must be chosen so that $\bar{y}_{j/i*} = r_j$. In this example, for y_2 to reach $r_2 = 200$, r_1 must be chosen as $r_2 G_1(0)/G_2(0) = 261.8$ rpm.

7.6 Acceleration and Deceleration Limiting

In addition to limits placed on the magnitudes of critical variables such as turbine temperature, shaft speeds, combustor pressure and engine pressure ratio, the core shaft acceleration must also be maintained between prescribed bounds. An upper bound is introduced to protect the engine against surge and stall, while the lower limit is introduced to provide safety against engine flame-out. Recalling (2.2), we see that core acceleration $\dot{N}_c$ depends on fuel flow, W_F. A traditional way to maintain core acceleration below its prescribed upper bound is simply to override the value of u_r calculated by the min-selected regulators, replacing it with a constant rate of zero pps/sec whenever the acceleration reaches its upper limit. Minimum acceleration is likewise maintained by replacing the rate produced by the max stage with $u_r = 0$ whenever the acceleration reaches its lower limit.

In CMAPSS-1, these operations are implemented by override switches triggered by $\dot{N}_c$, as shown in Figs. 7.13 and 7.14. The threshold value for $|\dot{N}_c|$ is 500 rpm/s. Note that a similar acceleration limiting scheme could, in principle, be applied to $\dot{N}_f$. When thrust is being controlled indirectly by a feedback loop on N_f, however, such scheme is not necessary, since reference ramps are usually commanded for this variable. Hence, fan acceleration should follow response specifications. When an EPR loop is established as a means to achieve thrust control, N_f and N_c may be regarded as upper-limited variables, and corresponding acceleration limiters included.
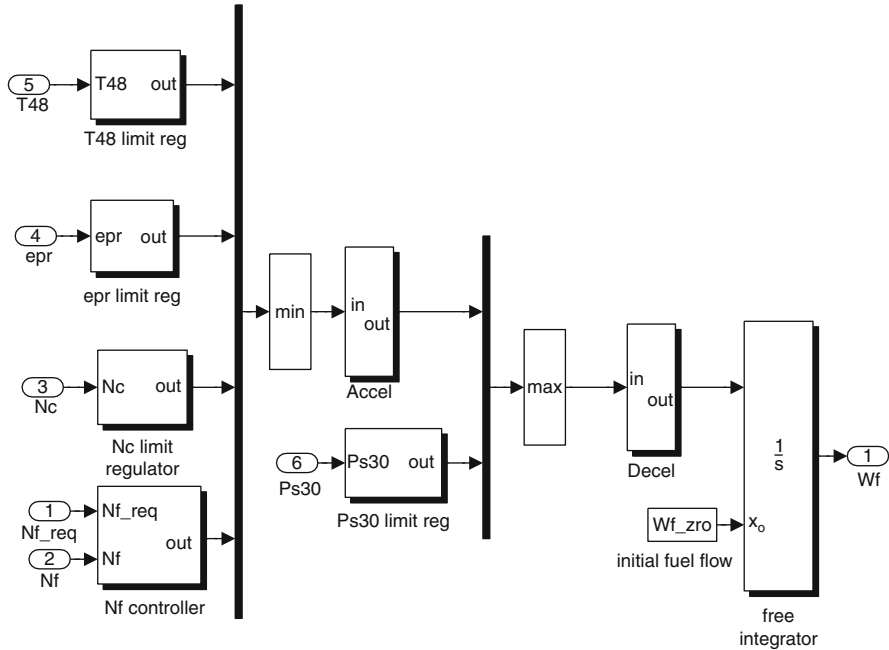
Fig. 7.13 Schematic of CMAPSS-1 min–max arrangement with acceleration and deceleration limiters
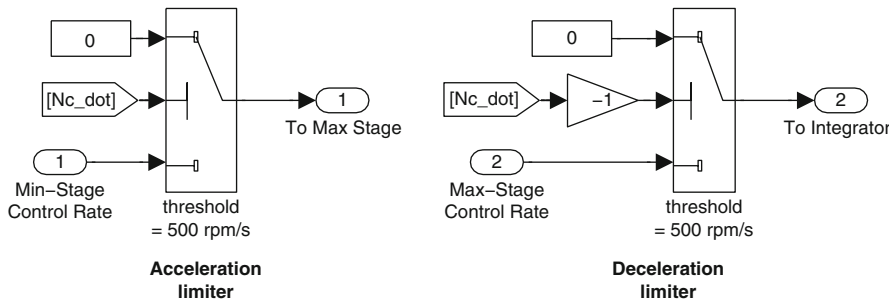

Fig. 7.14 Schematic of CMAPSS-1 acceleration and deceleration override switches

7.6.1 "N-Dot" Control and Acceleration Scheduling

The so-called "N-dot" control concept exploits the algebraic relationship between shaft accelerations and fuel flow, as observed in (2.1) and (2.2). In principle, if the inverse of functions f_1 and f_2 were available, one could compute values of fuel flow resulting in a desired instantaneous value for $\dot{N}_f$ or $\dot{N}_c$. In practice, no such inverses are available for real-time computations, and uncertain and unmeasurable time-varying parameters participate in the definitions of f_1 and f_2.

Since fuel flow is related to acceleration by an uncertain algebraic relationship, the latter may be controlled by establishing a PI loop using the former as control input. Assuming that good tracking properties are attainable, thrust control is achieved by providing adequate acceleration references, or *acceleration schedules*. These references are shaped so that their integral corresponds to a desirable shaft speed response. In addition, acceleration schedules may be used to introduce limit protections in critical engine variables. For more details on Ndot control, readers are referred to Link and Jaw [14] and Spang and Brown's survey [64].